

Copyright is owned by the Author of the thesis. Permission is given for a copy to be downloaded by an individual for the purpose of research and private study only. The thesis may not be reproduced elsewhere without the permission of the Author.

G R O U N D - L E V E L I N S O L A T I O N

I N T H E

U V - B S P E C T R A L R E G I O N

A THESIS PRESENTED IN PARTIAL FULFILMENT OF THE
REQUIREMENTS FOR THE DEGREE OF
MASTER OF SCIENCE
IN PHYSICS AT
MASSEY UNIVERSITY

by

BRUCE W. HARTLEY

1982

ABSTRACT

This thesis describes the design and construction of two instruments for use in isolating the ultraviolet parts of the Solar spectral irradiance at Earth's surface.

The first was a total UVA Pyranometer, which was undertaken to make preliminary investigations in the techniques of monitoring ultraviolet irradiances, as well as to provide useful data.

The main part of this thesis was the construction of a portable, easily operated, interference filter spectrophotometer to isolate the ultraviolet-B spectrum into five discrete 10 nm passbands. However, as further reading will describe, realisation of only the two longer wavelength passbands was made due to deviations from the ideal quasi-rectangular passbands of the interference filter spectral transmittance curves. Discussion of how these problems can be overcome is presented in the conclusion. An outline on how the incident spectral solar irradiance could be found, from the five passbands, is presented along with some preliminary data from the two operational channels. An overall accuracy of 15% was obtained for data obtained, with better accuracies, to 7%, attainable by stabilisation of the instrument power supplies and, therefore, output voltage.

ACKNOWLEDGEMENTS

Many thanks go to my supervisor Dr. R.K. Lambert for providing the topic about which this thesis is based, and providing many hours of interest and support during its construction. Also Mr E.R. Hodgson and the Massey University physics staff for assisting with ideas in the preliminary stages of the instrument constructions. The University workshop technicians provided invaluable assistance in supplying materials and equipment required in the design and construction, and the assistance of staff at the Physics and Engineering Laboratories, Gracefield, the New Zealand Meteorological Service, Wellington, and the Plant Physiology Division of the D.S.I.R., Palmerston North, in field testing and calibration of the instruments. Thanks also to my wife, Sharon, for her patience and support during the writing of this thesis, and to the typists Mrs Diane Burns, Mrs Rosalie Heap and Miss Kirsty Rutherford.

TABLE OF CONTENTS

	<u>Page</u>
Title	i
Abstract	ii
Acknowledgements	iii
Table of contents	iv
List of figures	v
List of tables	vii
Glossary	viii
<u>Chapter 1:</u> Introduction	1
<u>Chapter 2:</u> UVA Pyranometer	6
2.1 Description of the instrument	6
2.2 Cosine and linearity response	12
2.3 Calibration	14
2.4 Field test results	15
<u>Chapter 3:</u> UVB Filter wheel Pyranometer	19
3.1 Description of the instrument	21
3.2 Calculation of attenuation factors	29
3.3 Overall PMT sensitivity	36
3.4 Control electronics	40
3.5 Electronics test results	44
3.6 Calibration	48
3.7 Instrument cosine response	58
3.8 Data analysis procedure	60
3.9 Experimental data	61
<u>Chapter 4:</u> Conclusions	66
<u>Appendix I:</u> Vacuum photoemissive tube 92AV specifications	69
<u>Appendix II:</u> Photomultiplier tube 9656QB specifications	70
<u>Appendix III:</u> UVB instrument semiconductor components list	72
<u>Bibliography</u>	73

LIST OF FIGURES

		<u>Page</u>
1.1	Biological effects of UV radiation [1].	2
1.2	Bouger-Lambert diagrammatic representation.	2
2.1	UVA Pyranometer schematic.	7
2.2	UVA pyranometer filter transmittance and photocathode quantum efficiency.	10
2.3	Calculated spectral sensitivity curve of UVA pyranometer.	11
2.4	Cosine response of UVA pyranometer.	13
2.5	Linearity response of UVA pyranometer.	13
2.6	Comparison of UVA pyranometer to Eppley UVA radiometer.	16
2.7	Comparison of global UVA irradiance to global "total irradiance".	17
3.1	Functional block diagram of UVB instrument.	20
3.2	Collimator and PMT alignment.	22
3.3	Protective dome spectral transmittance.	24
3.4	UVB filter spectral transmittance curves.	25
3.5	Expanded scale, upper cut-off, transmittance curves.	26
3.6	Solar spectral irradiance curve from Robinson [1].	27
3.7	Visible filter spectral transmittance.	27
3.8	Calculated photocathode sensitivity.	30
3.9, 3.10	Calculated spectral irradiance transmitted by UVB filters.	32,33
3.11	Overall PMT sensitivity as a function of applied voltage.	37
3.12	Logarithm of normalised spectral sensitivity as a function of the logarithm of the normalised output voltage.	39
3.13	Electronics block diagram for UVB instrument.	41
3.14	Output voltage vs anode current for dark current monitor channel at constant EHT voltage.	46
3.15	PMT transfer function in the designed mode.	47
3.16	Calibration curves for UVB filter wheel instrument.	49
3.17	Apparatus set up for relative spectral sensitivity measurements.	51
3.18, 3.19	Normalised spectral response curves for interference filters, attenuators and PMT.	53,54
3.20	Normalised spectral response curves for complete instrument .	55
3.21	Apparatus layout for cosine response evaluation.	59

		<u>Page</u>
3.22	Instrument cosine response.	59
3.23, 3.24,		62,63
3.25	Normalised UVB data.	64

LIST OF TABLESPage

I	Ultraviolet wavelength classifications.	3
II	Transmitted spectral irradiance characteristics of UVB instrument filters.	34
III	Maximum allowable irradiance levels at the photocathode.	34
IV	Calculated maximum irradiance levels for UVB instrument.	35
V	Attenuators required for UVB filter channels.	35
VI	Spectral irradiance of 1000 watt tungsten halogen lamp.	56
VII	Experimentally determined calibration constant values.	57
VIII	Denormalisation factors for UVB experimental data.	61

GLOSSARY

a,b,c,	: Constants.
a_{λ}	: Optical thickness of atmosphere in the zenith direction.
A	: Attenuator and attenuation coefficient.
A_{aperture}	: Area of aperture.
A_D	: Area of diffuser that is irradiated.
A_k	: Area of photocathode that is irradiated.
c	: $3 \times 10^8 \text{ m s}^{-1}$.
C	: Calibration constant of UVA instrument.
dh	: Length of a column of atmosphere in the zenith direction.
ds	: Length of a column of atmosphere in the solar direction.
D_1	: Diode one.
D_n	: Dynode number n.
D_{λ}	: Spectral transmittance of the protective dome.
e	: Elementary charge.
e_o	: Output voltage of UVA instrument.
E	: Integrated irradiance over bandwidth $\lambda_2 - \lambda_1$.
EHT	: High voltage.
E_D	: Irradiance at the diffuser.
$E_{\text{instrument}}$: UVB instrument output for irradiance by the monochromator.
$E_{o,\text{instrument}}$: Normalising value of $E_{\text{instrument}}$.
E_k	: Irradiance at the photocathode.
E_n	: Total irradiance received by channel n.
$E_{n,o}$: Normalising value of E_n .
E_{output}	: Calibrating PMT output for irradiance by the monochromator.
$E_{o,\text{output}}$: Normalising value of E_{output} .

E_{pmt}	: Irradiance from the calibration monochromator.
$E_{\text{o,pmt}}$: Normalising value of E_{pmt} .
E_{solar}	: Total integrated solar irradiance.
$E_{\text{s,n}}$: Solar spectral irradiance of channel n.
E_{uVA}	: Integrated irradiance over the UVA band.
$E_{\text{k,max}}$: Maximum total irradiance allowable at the photocathode.
$E_{\text{o,n}}$: Total integrated irradiance of channel n after weighting of the incident spectral irradiance by the normalised spectral sensitivity of that channel.
$E_{\text{o},\lambda,\text{max}}$: Maximum spectral irradiance allowable at the diffuser.
E_{λ}	: Solar spectral irradiance of Earth's surface.
$E_{\lambda,n}$: Spectral irradiance of channel n.
$E_{\lambda,k,\text{max}}$: Maximum spectral irradiance allowable to the photocathode.
$E_{\lambda,\text{o},n}$: Approximation of the spectral irradiance of channel n.
F	: Filter.
F_{λ}	: Filter spectral transmittance.
FF_n	: Filter factor of channel n.
F	: Effective bandwidth of UVB instrument filters.
F_n	: Bandwidth of channel n filter.
G	: Gain of PMT in A/lm.
h	: Planck's constant.
i	: Total photocathode current.
i_{d}	: Dark current.
i_{k}	: Photoemissive current.
$i_{\text{k,max}}$: Maximum photocathode current allowable.
i_{o}	: Normalising value of i.
$i_{\lambda,k}$: PMT photocathode current for irradiance at wavelength λ .

I	: Integrated anode current over bandwidth ($\lambda_2 - \lambda_1$).
ICX	: Integrated circuit number X.
I_{Dark}	: PMT anode dark current.
$I_{o,\lambda}$: Incident monochromatic radiation intensity.
I_{λ}	: Transmitted monochromatic radiation intensity.
$I_{\lambda,A}$: PMT anode current for irradiance at wavelength λ .
K, K^1	: Calibration constants for the UVB instrument.
M	: PMT overall sensitivity in A/lm.
M_r	: Relative air mass.
P	: Denormalisation factor.
PMT	: Photomultiplier tube.
PT	: Photoemissive tube.
q	: Quartz diffusing disc.
Q_1	: Transistor number one.
Q_{λ}	: Photocathode quantum efficiency.
r	: Dimension of atmosphere particle.
r	: Source - detector distance.
r_o	: Normalising value of the source - detector distance.
R	: Resistance in ohms.
RC	: Resistor - Capacitor.
RX	: Resistor number X.
s_{λ}	: Spectral sensitivity of the photocathode.
S	: Integrated sensitivity over bandwidth ($\lambda_2 - \lambda_1$).
S_o	: Normalising value of S above.
S	: Solar position.
S_o	: Solar angle.
S_x	: Switch number X.
S_{λ}	: Total spectral sensitivity.
$S_{\lambda,n}$: Spectral sensitivity for channel n of the UVB instrument.
$S_{o,\lambda,n}$: Normalised values of $S_{\lambda,n}$.
T	: Total effective transmittance of UVB instrument diffuser, protective dome and collimator.
T_D	: Effective diffuser transmittance.

T_{Delay}	: Period of monostable delay pulse.
T_{sample}	: Period of monostable sample pulse.
UV	: Ultraviolet.
UVA	: Ultraviolet A radiation.
UVB	: Ultraviolet B radiation.
UVC	: Ultraviolet C radiation.
V	: UVB instrument output voltage.
V_0	: Normalising value of V.
V_{EHT}	: High voltage applied to the PMT.
Z	: Zenith position.
Z_0	: Zenith angle.
θ	: Angle from the normal of the diffuser surface. : Wavelength.
λ_0	: Wavelength of the irradiance $E_{0,\text{pmt}}$.
λ_1	: Lower limit of bandwidth.
λ_2	: Upper limit of bandwidth.
π	: Unit of angular measurement, $\pi = 3.141$.
ϕ_k	: Spectral radiant power at the PMT photocathode.
ϕ_{UVA}	: Integrated radiant power within the UVA band.
ϕ_λ	: Spectral radiant power at the photocathode.
Ω	: Solid angle subtended by the detector from the centre of the diffusing disc.

CHAPTER 1

Introduction

The importance of UV (ultraviolet) radiation that reaches Earth's surface is clearly seen when the action spectrum and effectiveness in the destruction of organic materials and biological tissues is observed. Fig:1.1 [1]* clearly illustrates this importance. Other effects of UV radiation include destruction of the genetic material (DNA), induction of skin cancers, eye inflammation and migration of melanin from lower to upper layers of skin as a form of protection known as tanning. Destruction of bacteria in skin diseases and sterilisation processes, and the production of vitamin D are some of the beneficial effects. Exposure of plants to intense UV is usually fatal, and lesser doses induce tumors, enhance genetic defects, stop photosynthesis and cause severe damage to outer leaf cells. Many insects use UV light as an "extended vision" for navigation, and food and predator recognition. This extended vision is exploited by humans in lures to capture insects for pest destruction or examination. Industrial organic materials such as rubbers and plastics break down after prolonged UV exposure and are rendered worthless.

In the erythemal region of the UV, which can cause severe sun-burning, it is interesting to observe the fallacies of some common beliefs about protection from the UV. Light colourful summer shirts can transmit up to 75% of the incident radiation, a one meter column of sea water transmits approximately 60% of radiation at 310 nm, and shady areas can receive large UV irradiances from diffuse sky radiation.

The UV spectrum from the sun has been subdivided into three sections of which two main classifications are presented in the literature.

* Numerals in square brackets refer to entries in the bibliography

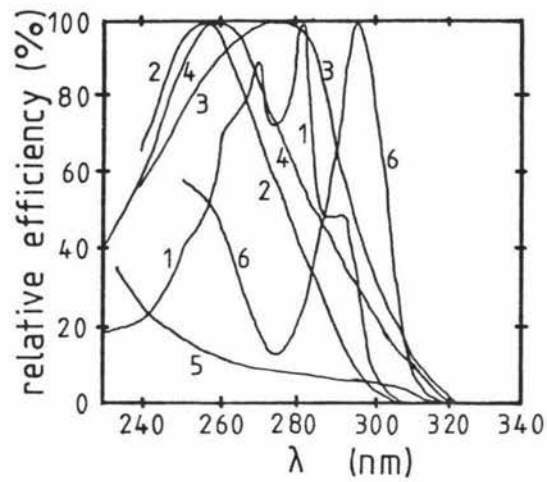


Fig:1-1 Biological effects of ultraviolet radiation[1].
 (1)Production of vitamin D,(2)bactericidal effects,
 (3)stoppage of tissue growth,(4)albumen coagulation,
 (5)haemolysis,(6)erythema.

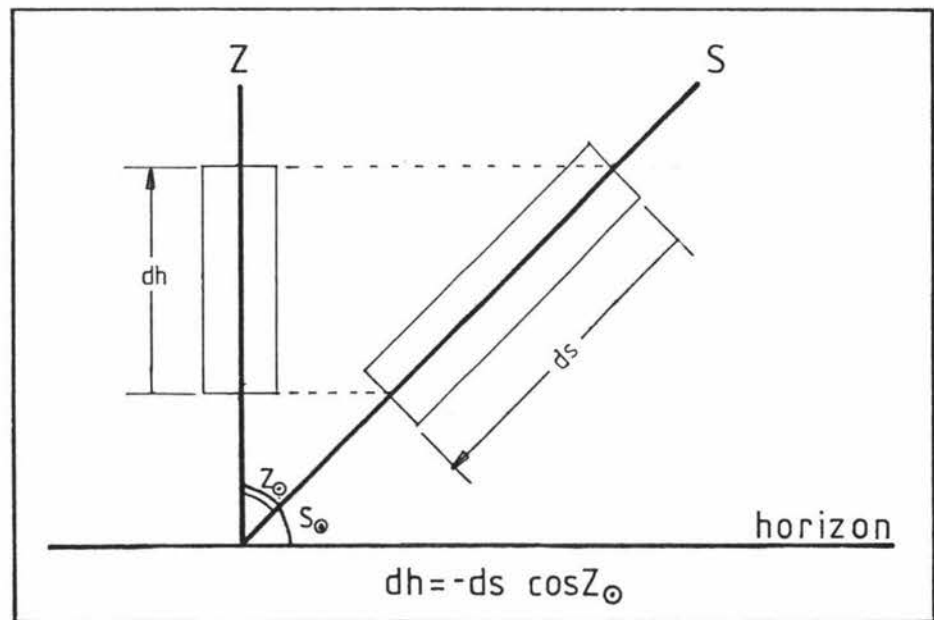


Fig:1-2 Bouger-Lambert law :diagramatic representation.

S:solar position

S_{\odot} :solar angle

Z:zenith position

Z_{\odot} :zenith angle

Table I

Ultra-Violet Wavelength classifications.

λ (nm), classification A [2,3]	λ (nm), classification B [4]
1-200 far UV	1-280 UVC
200-300 middle UV	280-320 UVB
300-400 near UV	320-400 UVA

Classification B, which is now the more commonly used, will be used in this thesis. The reasons for subdivision of the UV into the UVA, UVB and UVC become apparent when considering the radiation which reaches Earth's surface.

UVA: The atmosphere is relatively transparent to wavelengths of this region, and the radiation is weakly biologically active.

UVB: Transmission of this radiation is very dependent on the amount of ozone in the upper atmosphere. These wavelengths of radiation are responsible for erythema and most other biological effects.

UVC: No solar radiation of wavelength less than approximately 280 nm penetrates the atmosphere because of ozone and oxygen absorption.

Before reaching Earth's surface the Sun's radiation undergoes many modifications. Variation of the Earth-Sun distance causes an approximate 6% variation of the incident irradiance. Scattering and absorption in Earth's atmosphere, and reflection and radiation from Earth's surface also cause changes in the irradiance and polarization received at Earth's surface.

Scattering and Absorption

Prediction of atmospheric transmission is achieved by considering two columns of equal cross section in the atmosphere, one in the zenith direction and one in the solar direction.

The Bouger-Lambert law, equation (1.1), [1] expresses the relation between incident and transmitted radiation intensities.

$$\begin{aligned}
 I_{\lambda} &= I_{0,\lambda} \exp(-a_{\lambda} M_r) & (1.1) \\
 M_r &= \frac{-ds}{dh} \\
 &= \sec Z_{\theta}
 \end{aligned}$$

$I_{0,\lambda}$	Incident monochromatic radiation intensity on to column ds.
I_{λ} :	Transmitted monochromatic radiation intensity by column ds.
a_{λ} :	Optical thickness in zenith direction (extinction or attenuation coefficient).
M_r	Relative air mass of columns assuming constant atmospheric densities.

This theory neglects atmospheric curvature and refractive index changes between layers of the atmosphere at different temperatures and densities and, therefore, gives results which are valid only for high solar angles.

Scattering is responsible for the polarization of diffuse sky radiation, and the variation of scattering coefficients with wavelength gives a diffuse sky spectrum different from that of the direct radiation. This dependence of coefficient on wavelength is described by the Rayleigh and Mie relations and, for longer wavelengths, by geometrical optics. The criterion for Rayleigh scattering is that the characteristic dimension of the aerosol, r , obeys the condition $r \leq 0.1\lambda$, where λ is the wavelength of the radiation incident on the aerosol particle. When this is satisfied the coefficient is proportional to λ^{-4} . This illustrates why a clear diffuse Rayleigh sky is blue, and the thicker the optical path the more the blue light is scattered out of the direct beam. This is seen at sunset with a red sun and deep blue diffuse sky radiation. As the wavelength gets shorter (into the UV) the scattering coefficient increases, and experiments [5] indicate that as much as 60% of the radiation in the UVB is received from the diffuse sky. For larger particles, $0.1\lambda \leq r \leq 25\lambda$, the Mie theory describes the scattering, and for $r \geq 25\lambda$, geometrical optics can be used. With increasing particle size the scattering coefficient becomes less wavelength-dependent; the effect is seen in a whitening of smog, dust and cloud laden skies.

Absorption of UV radiation by atmosphere gases is of great importance because of the destructive effects that would be produced by an increase in the UV at Earth's surface. Most important of the atmospheric gases is ozone which lies in the upper atmosphere, with peak concentration occurring between 10 and 40 km altitude and decreasing up to 90 km [2]. Even though the amount of ozone is small in comparison to the total atmosphere, (several millimeters of ozone at standard temperature and pressure compared to 8 km of total atmosphere) it has very strong photo-chemical properties in which UV radiation is absorbed. The main absorption occurs in the Hartley bands which extend from 200 to 320 nm and affect the UVB reaching Earth's surface. The Huggins bands cover 320 to 360 nm and affect the UVA but with less absorption than the Hartley bands. It is the ozone absorption that is responsible for the sharp cut-off with decreasing wavelength of the radiation spectrum observed at Earth's surface.

The information presented here illustrates the need for data from routine monitoring instruments, to provide a base line from which predictions of the effects of changes in UV insolation can be made. It follows that reliable instruments are required to provide this data, and to date instrumentation has failed to meet the requirements of large scale, consistent, spectral measurements of the UV that reaches Earth's surface. In this thesis, two such instruments will be described which have the capability of providing this baseline data. In chapter 2 a UVA pyranometer is described. This instrument provides information on the total UVA irradiance incident on a flat surface. A filter wheel based instrument is described in chapter 3. The data from this instrument can provide information on the spectral distribution of the irradiance received on a flat surface in the UVB band.